Noise Fundamentals

Report submitted in partial fulfilment of the requirements for the P443-P444 Course by

Danush S
Roll Number: 1711048

to the

School of Physical Sciences
National Institute of Science Education and Research

April 3, 2021

Acknowledgements

I would be wrong if I said this report was solely my work, it is rather the collective effort of all the people I have interacted with and sought guidance from, during the entirety of the experiment duration. I start by thanking Dr. Kartik Senapati, Dr. Santosh Babu Gunda and Mr. Aman Upadhyay for their valuable input, guidance and time. I like to thank the lab assistants Mr. Sakthivel V. A and Mr. Pravakar Mallick for their support, without whom this experiment would have taken longer for its completion.

Abstract

This report consists of experiments done to understand and quantify two fundamental noises, namely Johnson noise and Shot noise. We empirically justified their existence and also looked at the theoretical derivations to the equations that govern them, and thus experimentally validated these equations. For Johnson noise, the linear dependence on resistance, bandwidth and temperature was validated. For shot noise, the linear dependence on photo-diode current and bandwidth was validated. An attempt to reduce the noise due to different components was made. Studies the gain-flatness of an amplifier and corrections for the same at high frequencies was done. We also showed a way to model and measure temperature of sub room temperatures through the setup that was used. Through these experiments, we also found the value of the Boltzmann's constant and the fundamental unit of charge, e. Further studies on the existence of sub-shot noise currents were also done.

Contents

List of Figures

List of Tables

Chapter 1

Introduction

Signals and signal processing are topics that can never be removed when you are engineering something that involves electrical components. And electronics have been part of any technological advances we have made since the past century, so we see that studying signals and how we can process them better would help impact an individual and improve their life to a great extent. In fact, we are going to a world that needs everything delivered quicker, accurately and more efficiently. For example, we tend to get agitated when we have access to only a slow internet connection. But faster internet connections would require information to be sent faster and more accurately. Sending information more accurately would mean we would have to reduce noise that would creep in, to as low as possible, so that we are still able to extract the data.

This experiment involves studying 2 fundamental noises that are intrinsic to any apparatus owing to the physical nature of the apparatus. Studies on noise is not restricted to electrical components (acoustics), but can even extend to any field that involves information. There are other kinds of noises like interference and technical noise, but we will not focus on these topics. As explained in [1], we'll observe noise sources that arise from the Second Law of Thermodynamics, and from the quantization of electrical charge. Noise sources like this display the characteristics of non-periodic, unpredictable, random waveforms, but nevertheless conforming, in their statistical properties, to universal laws. Fundamental noise is especially worthy of study, for at least two reasons. The first reason is that fundamental noise presents us with a physics-based limit on the degree to which we can measure in a given experiment. The second reason we care about noise is that it becomes possible to use noise to measure the values of some fundamental constants. Boltzmann's constant k_B can be determined from the voltage or Johnson noise of resistors; and the magnitude of the charge on the electron, e, can be determined from the current or shot noise of a photocurrent.

Before you continue, it is to be taken into consideration that Chapter 2 contains most of the pre-requisite theory that can explain the experiments performed, but further details of the experiments and additional theory is also explained under Chapter 3 along with the results.

Chapter 2

Theory

2.1 Johnson Noise

For any temperature above 0K, every resistor would display a voltage across itself even if there is no current passing through it. This emf that the resistor generates is referred to as Johnson noise (V_J). Of-course the mean voltage over time is zero since it fluctuates between positive and negative values, but mean $(V_J)^2$ is non-zero. Johnson noise arises due to thermal agitation of the charge carriers (usually the electrons) inside an electrical conductor at equilibrium, which happens regardless of any applied voltage.

The predicted value for $<V_J^2(t)>$ is given by:

$$< V_J^2(t) >= 4k_B RT\Delta f \tag{2.1}$$

where k_B is the Boltzmann's constant, T is the temperature of the resistor and Δf is the 'bandwidth' used in the measurement electronics. For derivation of Eqn. 2.1, see Appendix A. As explained in [1], The involvement of bandwidth Δf is a first hint that 'noise' is quite distinct from 'signal'. Everyone starts with 'd.c. signals', which have nothing but a sign and a value, in Volts. Then there are 'a.c. signals', which have a magnitude (perhaps specified by amplitude, or RMS value, or peak-to-peak excursion) but also a frequency, or a mixture of frequencies. But it is the essence of fundamental noise that it contains, or is composed of, all frequencies. In fact, the amount of energy we can get out of a 'noise source' depends on the range of frequencies to which we arrange to be sensitive, and this is the reason for the inclusion of the bandwidth-factor Δf in the expression above.

2.1.1 The Need to Study Johnson Noise and the Boltzmann's Constant

Studying Johnson noise would indeed help us reduce noises arising from resistors due to thermal fluctuations, but there is a more fundamental reason for why Johnson noise is so important. As told in [2], the kinetic theory of gases was successful to predict the equation of stat for a mole of ideal gas: PV = k_BNT where P is the pressure, V is the volume, T is the temperature of the system of gas we are studying. For some time, physicists did not know how to accurately measure N or k_B. But it was Johnson's and Nyquist's papers

that made us be able to measure the Boltzmann's constant. This experiment will also involve measuring k_B (See Section 3.6).

A link between the microscopic and macroscopic was reported by Johnson in 1928 in a paper paired in the Physical Review with one by H. Nyquist that provided a rigorous theoretical explanation based on the principles of classical thermal physics. Johnson had demonstrated experimentally that the mean square of the voltage across a conductor is proportional to the resistance and absolute temperature of the conductor and does not depend on any other chemical or physical property of the conductor. At first thought, one might expect that the magnitude of Johnson noise must depend in some way on the number and nature of the charge carriers. In fact Nyquist's theory involves neither e nor N . It yields a result in agreement with Johnson noise observations and a formula for the mean square of the noise voltage which relates the value of the Boltzmann constant to quantities that can be readily measured by electronic and thermometric methods.

2.2 Shot Noise

Shot noise is a type of noise that arises from charge quantization, which at first seems non-intuitive, but as one reads through this section, the origin behind this concept will be clearer and fascinating. Macroscopic electric currents will display noise, ie. random fluctuations about their average d.c. value, and that this noise is directly attributable to the microscopic 'graininess' of electric current. Just like Johnson noise, shot noise might be a nuisance, or a limiting factor in certain measurements but its existence makes possible the determination of a physical quantity. Here for shot noise, it is the magnitude of the value of 'e', the fundamental charge.

If one looks at the number of electrons passing through a wire, the uncertainty in the number of electrons would be ± 1 if the source of electrons produced electrons with perfect regularity. But if you have a current consisting of statistically-independent arrivals of entirely uncorrelated electrons, the average number of electrons arriving in time t would then be n, but the actual number on any particular trial would be subject to the same n $\pm\sqrt{n}$ 'counting statistics' that you'd get in radioactive decay or any other Poisson process. Here, $n = it/e$, where i is the magnitude of the current and e is the unit of charge. In this experiment we produce an electron current which follow Poisson statistics by bringing in a light source and photo-diode. The most persuasively independent electrons are photo-electrons, the more so if the light producing them is 'thermal' light. When those photons fall onto a photo-diode, it is a fair picture to think of each photon absorbed in the p-n junction as producing an electron-hole pair. The internal electric field of the junction separates that pair, and drives the electron through an external circuit as part of an electric current. We assume that the photons produced as statistically-independent (since they're independently produced, and thereafter non- interacting); what's not quite so obvious is that the photo-electrons thereby produced will create a current of still-statistically-independent electrons (given that electrons in a wire certainly can interact through their electric field with other electrons). But [1] later states that the photo-electrons which display full shot noise are produced independently by photon arrivals, and then are removed (by internal electric fields) from the detector's depletion region in so short a time that it becomes fair to think of the electrons as not interacting.

Please have a look at Appendix B to see how the standard deviation of a Poisson process

is derived!

Here are the consequences of those statistical fluctuations: Suppose we have in a time τ the arrival of n electrons on average, delivering an average charge of $Q = i_{dc}\tau$. Now there will be fluctuations in charge about this mean, with standard deviation $\sigma_Q = e\sqrt{n} = e(\frac{i_{dc}\tau}{e})^{1/2}$. Since current is charge per unit time, the instantaneous current i(t) will also show statistical fluctuations about its mean i_{dc} , with standard deviation $\sigma_i = \sigma_Q/\tau = (\frac{i_{dc}e}{\tau})^{1/2}$.

Then, as further explained in [1], since the standard deviation is defined as $< [i(t) - i_{\rm dc}]^2 >^{1/2}$, we see that the deviation from the average, $\delta i(t) \equiv i(t) - i_{\rm dc}$, has a mean-square value given by

$$< [\delta i(t)]^2 \rangle = i_{\rm dc} e/\tau$$

which is, in fact, a result for the mean-square noise in the current $i(t)$. That we can measure! The only complication in this simple derivation is to relate the effective measurement time τ to the bandwidth Δf of the measurement system, as previously defined. A low-pass filter of corner frequency $f_{\rm c}$, and a bandwidth approximately given by $\Delta f = f_{\rm c} - 0$, defines a time-scale of $(2\pi f_{\rm c})^{-1}$, which is approximately the time scale on which statistically-independent readings can be made. So we might expect a result near

$$< \delta i^2(t) > \approx i_{\rm dc} e/\tau = i_{\rm dc} e\,(2\pi f_{\rm c})^{+1}$$

In fact, the correct result has exactly of this character, but with different numerical constants; Schottky's prediction for the mean-square noise in a current of uncorrelated electrons is

$$< \delta i^2(t) > = i_{\rm dc} e(2\Delta f) = 2ei_{\rm dc}\Delta f \tag{2.2}$$

2.2.1 Sub-Shot Noise Currents

Existence of Johnson and Shot noise is shown in Chapter 3 by designing certain experiments, this section is to empirically see that one can produce currents whose fluctuations are smaller than the standard shot-noise prediction. The immediate implication of such an observation is that electrons in such a circuit are not moving independently and at random, but instead in some more nearly regular way. As explained in [1], the mechanism for this enhanced regularity seems to be the Coulombic interactions of the whole cloud of electrons that is diffusing by collisions through the resistor. If electrons do interact this way, the previous argument of statistically-independent arrivals would fail. By contrast, the photo-electrons which you've already seen displaying full shot noise are produced independently by photon arrivals, and then are removed (by internal electric fields) from the detector's depletion region in so short a time that it becomes fair to think of the electrons as not interacting.

Chapter 3

Experiments Conducted and Subsequent Results

This chapter looks into the set of experiments conducted over a period of six weeks. The set of experiments performed can be divided into 9 parts:

1. Empirical validation of Johnson noise and Amplification noise
2. Dependence of Johnson Noise on resistance
3. Dependence of Johnson Noise on bandwidth
4. Measurement of Boltzmann's constant
5. Temperature dependence of Johnson Noise
6. Dependence of shot noise on photo-diode current and bandwidth
7. Measurement of e
8. Diagnosing proper high-frequency behavior
9. Sub-Shot Noise

As stated in Chapter 1, additional theory behind any experiment would be explained along the way, if necessary.

3.1 Setups and Apparatus Used

There are 2 main devices that are constantly used throughout this experiment (made by TeachSpin, Inc.): the High Level Electronics (HLE) box and the Low Level Electronics (LLE) box. Pictures of the same are showin in Fig. 3.1. We will be opening the LLE box everytime we need to change the circuits we are using. The interior of the same is as seen in Fig. 3.2a. For temperature measurement we will also need additional setup that includes a Dewar for housing Liquid Nitrogen and corresponding circuits (See Fig. 3.2b.

(a) (b)

Figure 3.1: Image of the (a)HLE and (b)LLE boxes used.

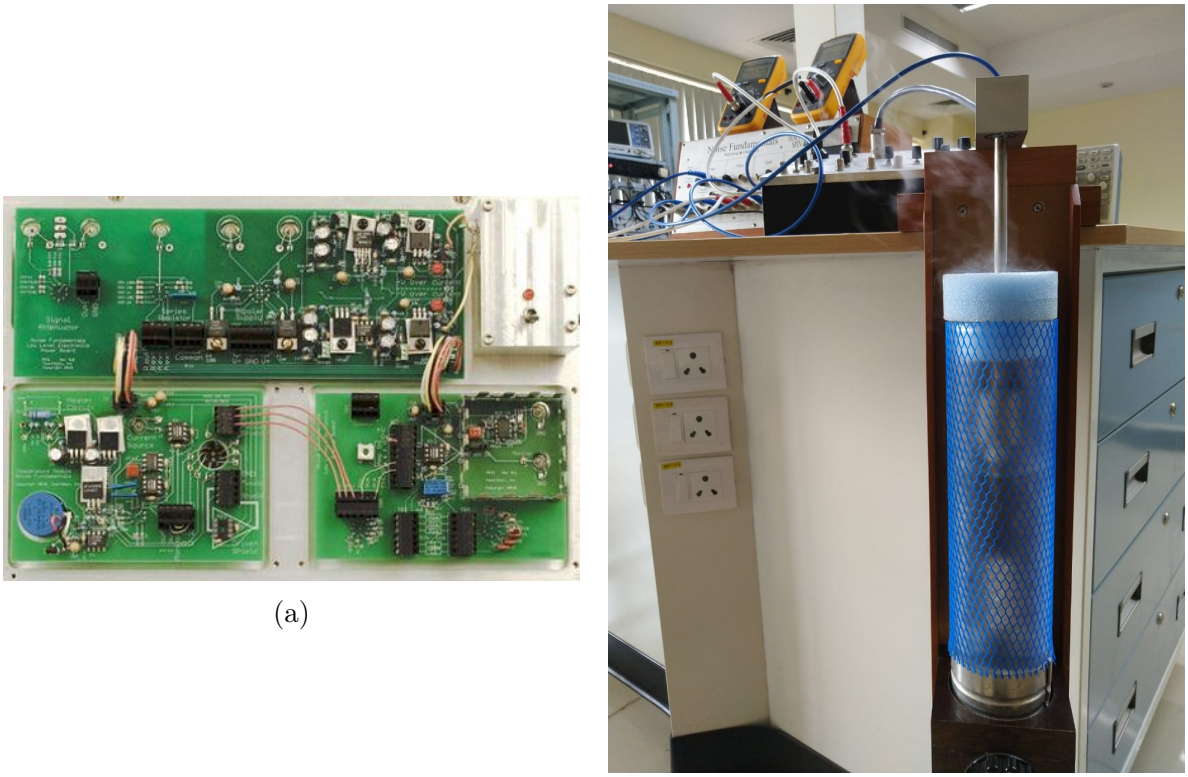

(a) (b)

Figure 3.2: Image of the (a) circuits on the inside of the LLE box and (b) temperature-measurement setup.

TeachSpin, Inc. also provides us with 2 boxes that includes resistors, photodiodes, LEDs, etc. Aside from the TeachSpin equipment, we will need a frequency generator, digital multimeters, an oscilloscope, BNC cables and jumper wires. Additional changes and required circuit connections will be shown in the subsequent sections of experiments. All relevant details are very neatly explained in the TeachSpin Manual [1].

3.2 Empirical Validation of Johnson Noise and Amplification Noise

This section involves looking to see if the voltage we obtain has characteristics of a noise, to see if the magnitude of the noise voltage is similar to what the theory predicts and also to learn how to calculate amplification noise.

We would require to build a circuit shown in Fig. 3.3 using the (Low Level Electronics) LLE box. We then connect the pre-amp output to a band-pass (0.1-100kHz) and then the gain (x300) connection of the (High Level Electronics) HLE box. We then take the gain output and connect it to an Oscilloscope. Using Eqn. 2.1, we expect the magnitude of voltage of the Johnson noise should be about 2.5V (rms) (the LLE box would have a gain of 600), which is as seen in Fig. 3.4a.

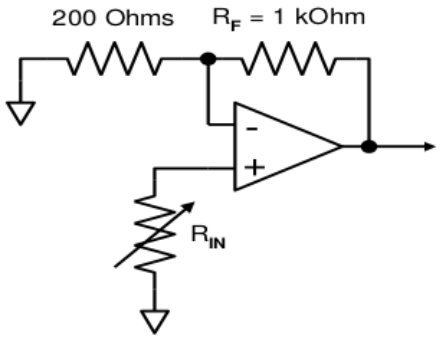

Figure 3.3: Schematic diagram of a circuit to "see Johnson noise". $R_{IN} = 100k\Omega$. Source: [1]

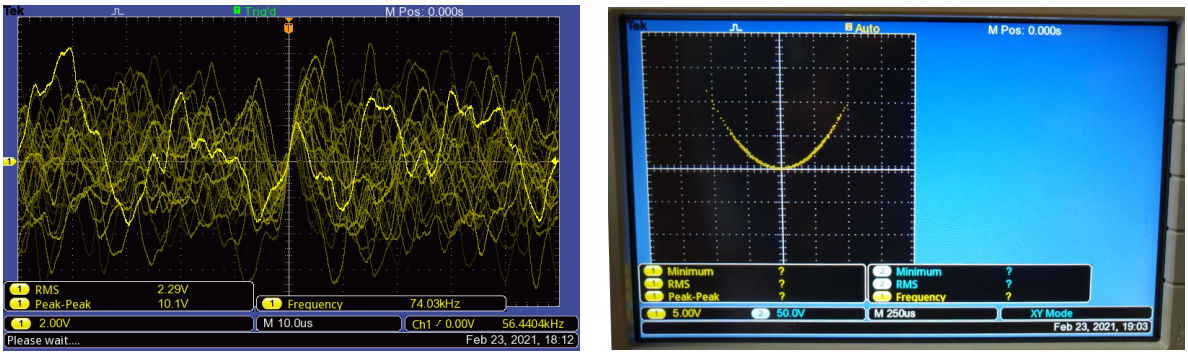

(a) (b)

Figure 3.4: (a) Oscilloscope output of the "Seeing Johnson noise" (b) Oscilloscope XY display output with input voltage on X-channel and squarer output on Y-channel.

We see that Fig. 3.4a has characteristics of how a noisy supply would look like. In addition to this, we observed that changing R_{in} changes the magnitude of the final voltage we are observing, thus giving us a hint that the noise we are observing depends on the resistances we are utilising. We also realise that once we prove that the noisy voltage we are observing, linearly depends on temperature, resistance used and the frequency bandwidth, we can confidently say that the voltage we are observing stems from Johnson noise as the experiment aligns with what the theory predicts (specifically, Eqn. 2.1).

[1] states that there is a gain factor of 6 (If R_f is set to 1kΩ before the additional amplification gain of 100. The reason for this can be found out when one works out the output voltage of the opamp in Fig. 3.3, taking voltage produced by R_{IN} as V_J.

Now moving on to the amplification noise, which can emerge due to the amplifier which is being used in the circuit and would have a noise voltage associated with it. The problem we're now going to address is tracing noise back to a source, because here we have to consider the possibility that some of the noise might be due to the amplifier chain which follows it. Since this 'amplifier noise' is just as featureless and random as the resistor's Johnson noise, fortunately there is a way to separate their effects if we can assume that the amplifier noise does not depend on the source resistor's value.

Let $V_J(t)$ be the instantaneous noise voltage from the source resistor, and let $V_N(t)$ be the instantaneous noise voltage apparently present at the input of the amplifier. That is to say, $V_N(t)$ is a model for a noise emf which, applied to the input of an ideal noiseless amplifier, would match the noise actually observed at the output of the real amplifier, driven only by its internal noise. If the gain of the amplifier is G, then its output will be

$$V_{\text{out}}(t) = G\left[V_{\text{J}}(t) + V_{\text{N}}(t)\right]$$

and the Mean-Square (M.S) of this output will be

$$\begin{aligned} < V_{\text{out}}^2(t) > &= G^2 < \left[V_{\text{J}}(t) + V_{\text{N}}(t)\right]^2 > \\ &= G^2\left\{< V_{\text{J}}^2(t) > + 2 < V_{\text{J}}(t) \cdot V_{\text{N}}(t) > + < V_{\text{N}}^2(t) >\right\} \end{aligned}$$

There's a 'cross term' in this expression, the time average of the product $V_{\text{J}}(t) \cdot V_{\text{N}}(t)$, but this time average is zero. The reason is that $V_{\text{J}}(t)$ and $V_{\text{N}}(t)$ can be safely assumed to be uncorrelated, arising as they do from distinct physical mechanisms in two different objects. So when $V_{\text{J}}(t)$ happens to be positive, the amplifier noise $V_{\text{N}}(t)$ is just as likely to be negative as it is positive; thus the product of the two factors is also as likely to be negative as positive. That's why the absence of correlation enforces a zero for the time average of the product. But that fact leaves

$$< V_{\text{out}}^2(t) >= G^2\left\{< V_{\text{J}}^2(t) > + 0 + < V_{\text{N}}^2(t) >\right\}$$

which says that mean-square voltages from uncorrelated sources are simply additive. In particular, it gives us a way to measure the amplifier noise - - we just change temporarily to a configuration in which the Johnson-noise term in this sum is negligible. Theory says that a choice of $R = 0$ for source resistance would give $< V_{\text{J}}^2(t) >= 0$, but in practice, it suffices to use the $R = 1\Omega$ or 10Ω settings for giving a $< V_{\text{J}}^2(t) >$ which is small enough that the result is a good measure of the amplifier noise, $< V_{\text{N}}^2(t) >$.

We calculated amplification noise for two HLE gains (x1000 and x1500). For both setups, we used $R_f = 1\text{k}\Omega$, frequency bandwidth 0.1-100 kHz, LLE gain 600, time constant = 1s,

conducted at room temperature (295K). On further passing it through a squarer, we get $V_{out}(t) = \frac{[V_{in}(t)]^2}{10V}$, where 10V is a scaling factor. See Fig. 3.4b to observe that the squarer is working since we expect a parabola as the output.

R_{IN} (Ω)	$<V_{sq}>$(V)	$<V_J^2 + V_N^2>(V^2)$
1	0.244	6.778E-12
10	0.245	6.806E-12
100	0.251	6.972E-12
1000	0.312	8.667E-12
10000	0.93	2.583E-11

Table 3.1: Observations: Calculating amplification noise for HLE gain 1000.

R_{IN} (Ω)	$<V_{sq}>$(V)	$<V_J^2 + V_N^2>(V^2)$
1	0.551	6.802E-12
10	0.552	6.815E-12
100	0.567	7.000E-12
1000	0.704	8.691E-12

Table 3.2: Observations: Calculating amplification noise for HLE gain 1500.

Another interesting experiment to perform, that we failed to do in the time we had, is to see how amplification gain changes with gain. From Tables 3.1 and 3.1 ($<V_J^2 + V_N^2>$ entry corresponding to $R_{IN} = 1\Omega$ is the amplification noise) the amplification noise turns out to be very close, but intuition would tell us that this noise should increase with the gain we are using.

Ideally we make an appropriate plot and obtain the intercept to find the amplification noise (i.e at $R_{IN} = 0\Omega$), but we see from Fig. 3.5 and 3.6 that the intercept and the voltage at $R_{IN} = 1\Omega$ is almost the same.

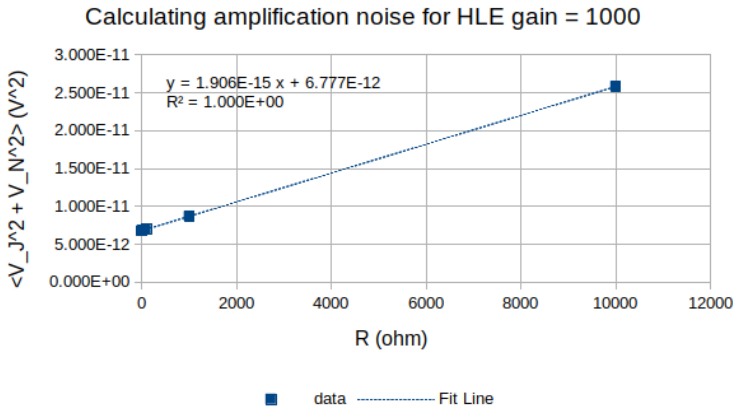

Figure 3.5: $<V_J^2 + V_N^2>$ vs R_{IN} plot for HLE gain = 1000.

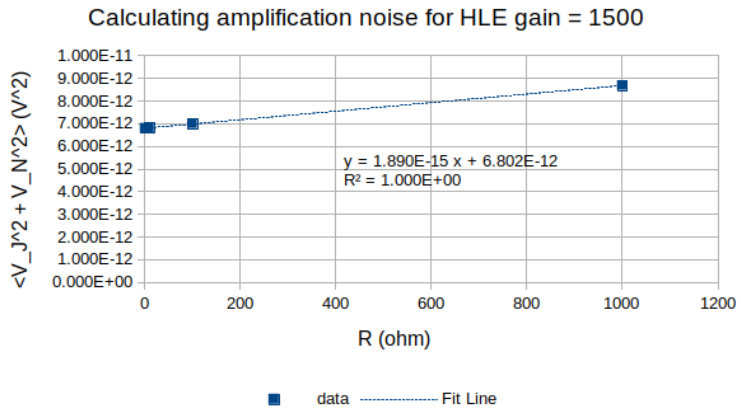

Figure 3.6: $<V_J^2 + V_N^2>$ vs R_{IN} plot for HLE gain = 1500.

The slope and intercept of the fitted line in Fig. 3.5 are $(1.905\times10^{-15} \pm 1.239\times10^{-18})\frac{V^2}{\Omega}$ and $(6.777\times10^{-12} \pm 5.57\times10^{-15})V^2$ respectively. The slope and intercept of the fitted line in Fig. 3.6 are $(1.89\times10^{-15} \pm 9.26\times10^{-18})\frac{V^2}{\Omega}$ and $(6.802\times10^{-12} \pm 4.653\times10^{-15})V^2$ respectively.

The reason we observed amplification noise for two gains is to see the dependence of one on the other, and we see that there is a slight difference (of order of 0.03E-12) between the voltage of the noises for different gains.

3.3 Dependence of Johnson Noise on Resistance

According to Eqn. 2.1, we should observe a linear dependence between the resistance and Johnson noise. To show this dependence, we use the circuit as shown in Fig. 3.7.

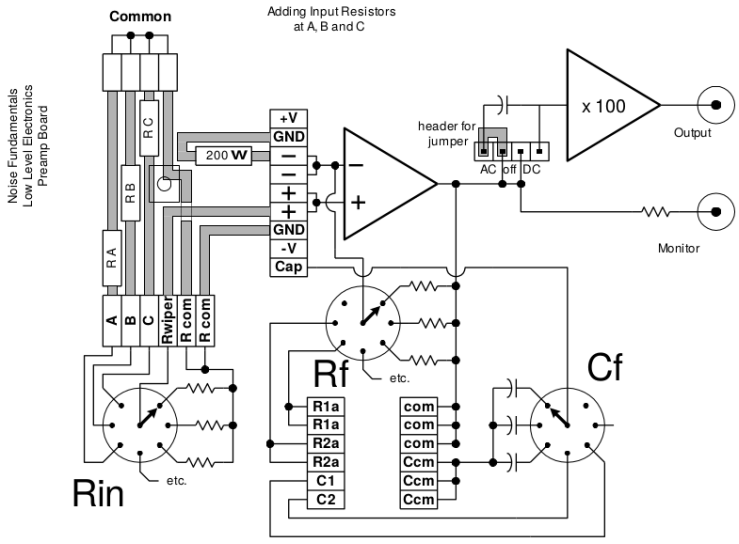

Figure 3.7: Electrical circuit for Johnson noise vs R. Source: [1]

As done in the previous section, we again obtained plots for 2 HLE gains (x1000 and x1500). For both setups, we used $R_f = 1k\Omega$, frequency bandwidth 0.1-100 kHz, LLE gain 600, time constant = 1s, conducted at room temperature (296K).

R_{IN} (Ω)	$<V_{sq}>$(V)	$<V_J^2 + V_N^2>$(V^2)	$<V_J^2>$(V^2)
1	0.243	6.750E-12	-2.700E-14
10	0.245	6.806E-12	2.856E-14
30	0.245	6.806E-12	2.856E-14
100	0.251	6.972E-12	1.952E-13
300	0.264	7.333E-12	5.563E-13
1000	0.312	8.667E-12	1.890E-12
3000	0.45	1.250E-11	5.723E-12
10000	0.931	2.586E-11	1.908E-11

Table 3.3: Observations: Corrected M.S Johnson noise vs R_{IN} for HLE gain 1000.

R_{IN} (Ω)	$<V_{sq}>$(V)	$<V_J^2 + V_N^2>$(V^2)	$<V_J^2>$(V^2)
1	0.551	6.802E-12	3.469E-15
10	0.553	6.827E-12	2.816E-14
30	0.556	6.864E-12	6.520E-14
100	0.566	6.988E-12	1.887E-13
300	0.597	7.370E-12	5.714E-13
1000	0.705	8.704E-12	1.905E-12

Table 3.4: Observations: Corrected M.S Johnson noise vs R_{IN} for HLE gain 1500.

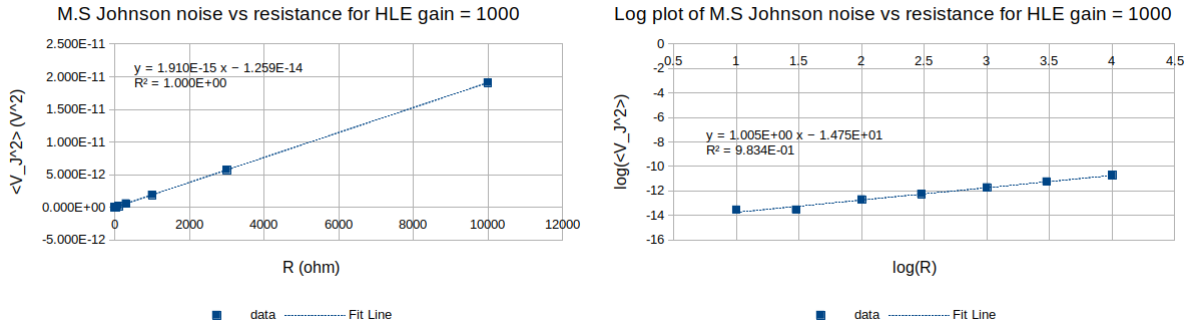

(a) (b)

Figure 3.8: (a)M.S Johnson noise vs R_{IN} plot, (b)Log plot of M.S Johnson noise vs R_{IN} for gain 1000.

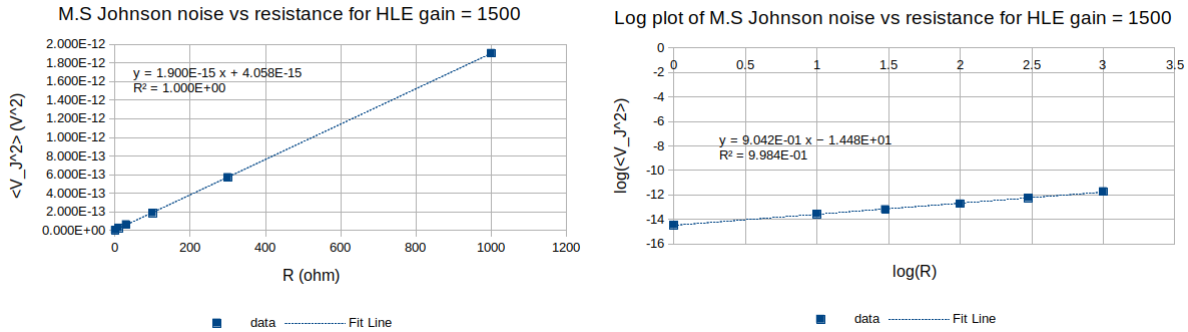

(a) (b)

Figure 3.9: (a)M.S Johnson noise vs R_{IN} plot, (b)Log plot of M.S Johnson noise vs R_{IN} for gain 1500.

The slope and intercept of the fitted line in Fig. 3.8a are $(1.909\times10^{-15} \pm 1.675\times10^{-18})\frac{V^2}{\Omega}$ and $(-1.234\times10^{-14} \pm 6.215\times10^{-15})V^2$ respectively. The same for Fig. 3.8b are 1.005 $\pm$ 0.058 and -14.75 $\pm$ 0.1567 respectively.

The slope and intercept of the fitted line in Fig. 3.9a are $(1.9\times10^{-15} \pm 5.337\times10^{-18})\frac{V^2}{\Omega}$ and $(4.05\times10^{-15} \pm 2.286\times10^{-15})V^2$ respectively. The same for Fig. 3.9b are 0.904 $\pm$ 0.018 and -14.48 $\pm$ 0.035 respectively.

We see that Table 3.4 does not have the same number of entries compared to Table 3.3, this is because for higher R_{IN} values, the gain had to be changed to keep $<V_J^2 + V_N^2>$ under 1V. We see a similar situation in Tables 3.1 and 3.2.

3.4 Dependence of Johnson Noise on Bandwidth

Eqn. 2.1 predicts that Johnson noise would also depend on the bandwidth of frequencies. The intuition behind the same is that since Johnson noise is white noise, it can be expected to present at all frequencies. When we limit the measurement to a range of frequencies, the voltage reduces proportionally.

Another thing to keep in mind is that we might first think that the bandwidth should be given by $|f_2 - f_1|$ where f_1 and f_2 are the corner frequencies of the high and low pass filters used. This is a decent approximation, but subject to significant corrections. It is $|f_2 - f_1|$ when we have a 'brick wall' like model of the filtering process, in which the filter sections together gave gain factor = 1 for $f_1 < f < f_2$, but gain = 0 elsewhere. But real filters do not have such sharp-edged characteristics, which is why define effective bandwidth to accommodate for this shift from ideal filters to a more realistic value.

Another way to see this is through entries in Table 3.5, where some entries have 0 bandwidth, where we expect no signal to pass through, hence give us 0 M.S Johnson noise but we get a finite positive value instead. The same entry would have a finite positive effective bandwidth, hence explaining the non-zero M.S Johnson noise.

The circuit is the same as shown in Fig. 3.7. We set R_{IN} = 10kΩ, R_f = 1kΩ, time constant = 1s at room temperature (298K).

Bandwidth (Hz)	Effective Bandwidth (Hz)	$<V_J^2>(V^2)$
320	355	5.667E-14
300	333	5.444E-14
230	258	4.556E-14
30	105	1.778E-14
0	9	0.000E+00
0	0.4	0.000E+00
990	1100	1.822E-13
970	1077	1.778E-13
900	1000	1.667E-13
700	784	1.300E-13
0	278	4.778E-14
0	28	5.556E-15
3290	3654	6.156E-13
3270	3632	6.156E-13
3200	3554	6.044E-13
3000	3332	5.644E-13
2300	2576	4.389E-13
300	1051	1.833E-13
9990	11096	1.852E-12
9970	11074	1.852E-12
9900	10996	1.840E-12
9700	10774	1.802E-12
9000	9997	1.679E-12
7000	7839	1.321E-12
32990	36643	6.259E-12
32970	36620	6.272E-12
32900	36543	6.247E-12
32700	36321	6.210E-12
32000	35543	6.074E-12
30000	33324	5.728E-12
99990	111061	1.933E-11
99970	111039	1.928E-11
99900	110961	1.925E-11
99700	110739	1.928E-11
99000	109961	1.914E-11
97000	107740	1.886E-11

Table 3.5: Observations: M.S Johnson noise (amplification noise corrected) for different bandwidths (and subsequent effective bandwidths).

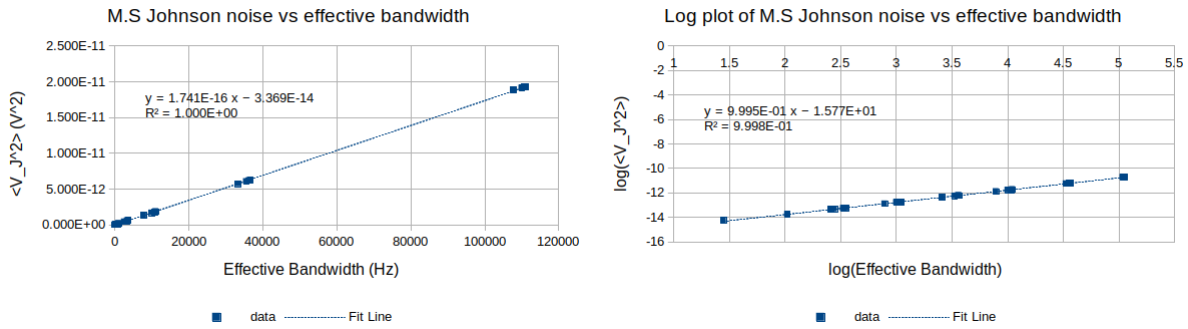

(a) (b)

Figure 3.10: (a)M.S Johnson noise vs effective bandwidth plot, (b)Log plot of M.S Johnson noise vs effective bandwidth.

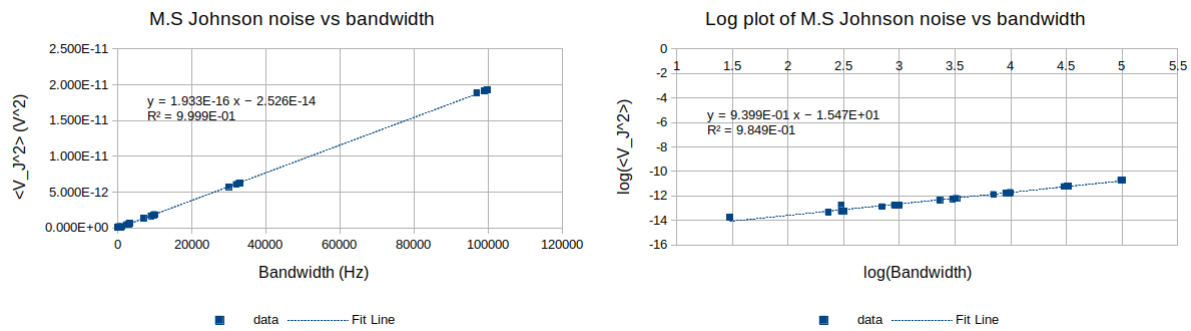

(a) (b)

Figure 3.11: (a)M.S Johnson noise vs bandwidth plot, (b)Log plot of M.S Johnson noise vs bandwidth.

The slope and intercept of the fitted line in Fig. 3.10a are $(1.741\times10^{-16} \pm 2.034\times10^{-19})\frac{V^2}{Hz}$ and $(-3.369\times10^{-14} \pm 9.669\times10^{-15})V^2$ respectively. The same for Fig. 3.10b are 1 ± 0.003 and 15.77 ± 0.032 respectively.

The slope and intercept of the fitted line in Fig. 3.11a are $(1.933\times10^{-16} \pm 2.649\times10^{-19})\frac{V^2}{Hz}$ and $(-2.527\times10^{-14} \pm 1.134\times10^{-15})V^2$ respectively. The same for Fig. 3.11b are 1.048 ± 0.024 and 16.26 ± 0.283 respectively.

We see that although the difference is subtle, the plot of effective bandwidth vs M.S Johnson noise has lesser least square error than the bandwidth vs M.S Johnson noise plot.

3.5 Temperature Dependence of Johnson Noise

This section is to verify the linear dependence of Johnson noise on temperature (two-temperature Johnson-noise measurement) and to perform an experiment to generate a model to measure temperatures from 77K to room temperature (temperature measuring and modelling. The set of experiments performed in this section would involve the use of the 'thermal probe' and its associated Dewar vessel. Together they make it possible to measure Johnson noise from a source resistor as a function of its temperature T. The system is designed for use with liquid nitrogen (LN_2) as a coolant, and an electrical heater allows exploration above that base temperature. The probe is suited for use in the (77 - 400)K range. The lower end is set by the normal boiling point of LN_2; the upper end (which is 400K) is set by temperature limits of wires and components in the probe head, and is enforced by the limited power available to the heater. The thermal probe consists of 3 resistors which can be replaced inside a shielding sleeve (remote resistors). This is meant to be immersed in a system with set temperature in order to measure the property of the resistors at the given temperature. Upon measuring we found the values of the 3 resistors to be $R_a = 10.2\Omega$, $R_b = 9.96k\Omega$ and $R_c = 100.5k\Omega$. The circuit for performing experiments in this section is as seen in Fig. 3.12. We will refer to the resistors in the LLE as local resistors.

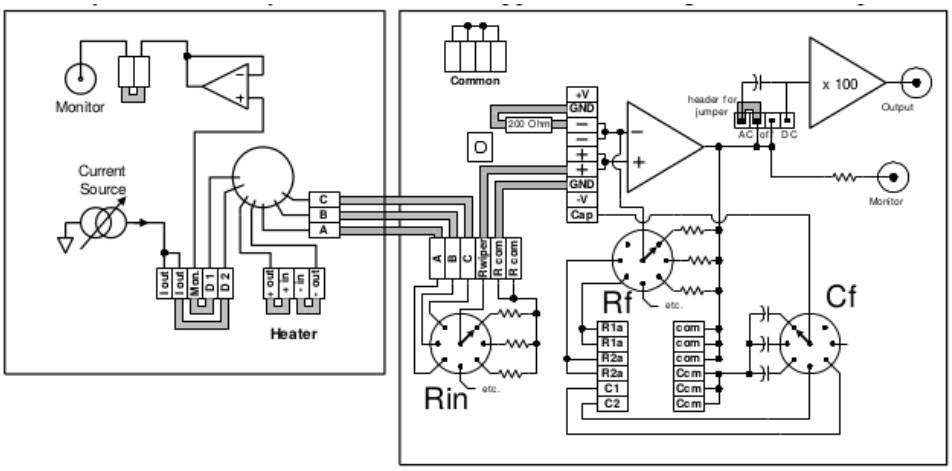

Figure 3.12: Circuit to measure temperature dependence of Johnson noise. Source: [1]

3.5.1 Two-Temperature Johnson-Noise Measurement

For the experiment in this section, we used, $R_a = 10.2\Omega$, $R_b = 9.96k\Omega$, $R_c = 100.5k\Omega$, $R_f = 1k\Omega$, and a $100\mu A$ current source.

High pass (kHz)	Low pass (kHz)	$<V_{sq}>$for different R_{INS} (V)						Gain	$<V_J^2>$for different R_{INS} (V^2)	
		10Ω local	10Ω remote	10kΩ local	10kΩ remote	100kΩ local	100kΩ remote		10kΩ remote	100kΩ remote
1	10	0.02	0.02	0.081	0.08	0.616	0.454	600000	1.667E-12	12.056E-12
3	33	0.025	0.025	0.099	0.093	0.705	0.275	360000	5.247E-12	19.290E-12
3	10	0.015	0.015	0.063	0.062	0.486	0.331	600000	1.306E-12	8.778E-12

Table 3.6: Observations: Two-temperature Johnson-noise measurement at room temperature (296K).

High pass (kHz)	Low pass (kHz)	$<V_{sq}>$for different R_{INS} (V)			Gain	$<V_J^2>$for different R_{INS} (V^2)	
		10Ω remote	10kΩ remote	100kΩ remote		10kΩ remote	100kΩ remote
1	10	0.02	0.049	0.264	600000	805.556E-15	6.778E-12
3	33	0.025	0.048	0.125	360000	1.775E-12	7.716E-12
3	10	0.015	0.028	0.109	600000	361.111E-15	2.611E-12

Table 3.7: Observations: Two-temperature Johnson-noise measurement at 77K.

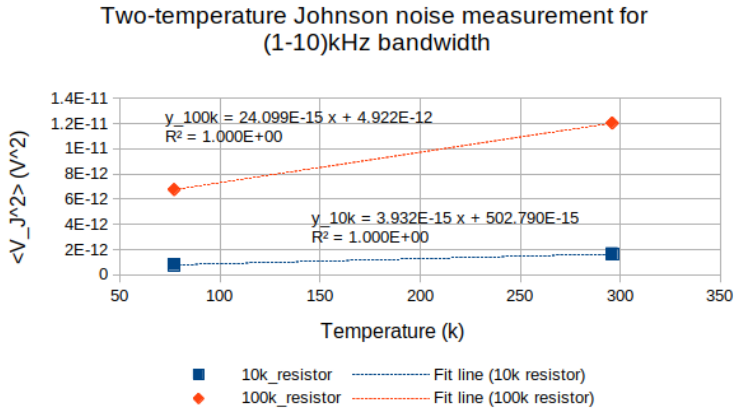

Figure 3.13: M.S Johnson noise vs Temperature for (1-10)kHz bandwidth.

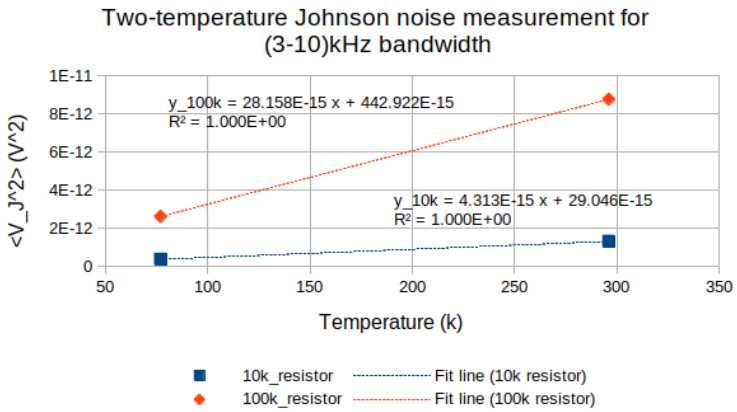

Figure 3.14: M.S Johnson noise vs Temperature for (3-10)kHz bandwidth.

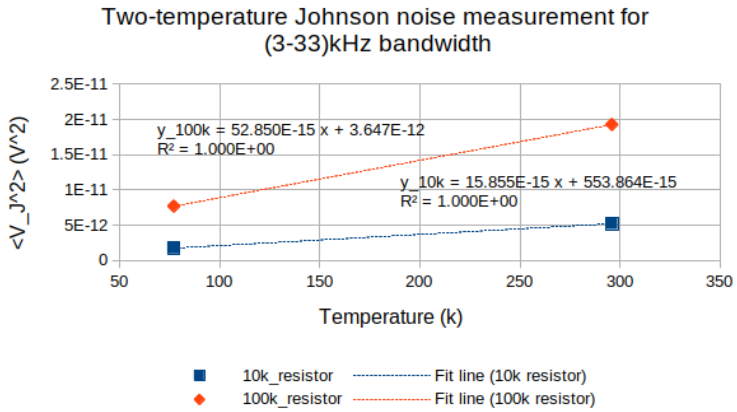

Figure 3.15: M.S Johnson noise vs Temperature for (3-33)kHz bandwidth.

For Figures 3.13, 3.14 and 3.15, there are only 2 points in each graph, hence the error in slope and intercept is 0.

3.5.2 Temperature Measuring and Modelling

The trans-diode connection simulates a p-n junction diode with an ideality parameter η=1, so that to a fine approximation we can write the diode current i as a function of potential difference ΔV and temperature T as (from the manual):

$$i(\Delta V, T) = i_0(T)\left[\exp\left(e\Delta V/\left(k_{\mathrm{B}}T\right)\right) - 1\right]$$

Taking log on both sides and dropping the term (-1) as it is very small, we get:

$$\ln i(\Delta V, T) = \ln i_0(T) + e\Delta V/\left(k_{\mathrm{B}}T\right)$$

or, $\Delta V = \left(k_{\mathrm{B}}T/e\right)\left[\ln i(\Delta V, T) - \ln i_0(T)\right]$. If we measure then noise ΔV_{10i} at 10i and ΔV_i at current i, we have

$$\Delta V_{10} = \left(k_{\mathrm{B}}T_{\mathrm{x}}/e\right)\left[\ln(10i) - \ln i_0\left(T_{\mathrm{x}}\right)\right]$$

and

$$\Delta V_1 = \left(k_{\mathrm{B}}T_{\mathrm{x}}/e\right)\left[\ln(1i) - \ln i_0\left(T_{\mathrm{x}}\right)\right]$$

On further modification, this yields us

$$T_{\mathrm{x}} = [e\delta(\Delta V)/k_{\mathrm{B}}]\,(\ln 10)^{-1}$$

or

$$T_{\mathrm{x}} = 5.04\mathrm{k/mV}\Delta\mathrm{V}$$

In this experiment, we took the voltage measurements at three different current values (1A, 10A, 100A) and we will call them as V1, V10 and V100 respectively. These readings will help us calculate two values of the temperature of the setup. Averaging the two values, we can get a better value.

For the experiment in this section, we used R_f = 1kΩ (G1 = 600), R_A = 10.2 Ω, R_B = 9.96kΩ and bandwidth (3-33)kHz.

At constant temp (mV)			V_{sq} for R_A and R_B (V)		Gain	Average temperature
V1	V10	V100	R_A	R_B		(K)
933	952	972	0.167	0.309	1500	98.28
906	927	948	0.167	0.324	1500	105.84
856	881	905	0.167	0.351	1500	123.48
851	877	902	0.167	0.356	1500	128.52
844	870	896	0.167	0.358	1500	131.04
843	868	894	0.167	0.361	1500	128.52
835	862	888	0.167	0.363	1500	133.56
827	855	881	0.167	0.366	1500	136.08
816	844	872	0.167	0.373	1500	141.12
808	837	866	0.167	0.377	1500	146.16
802	831	860	0.167	0.38	1500	146.16
787	817	847	0.167	0.386	1500	151.2
775	806	837	0.167	0.394	1500	156.24
756	791	823	0.167	0.401	1500	168.84
731	765	800	0.167	0.415	1500	173.88
720	756	790	0.167	0.417	1500	176.4
700	737	773	0.167	0.428	1500	183.96
680	718	755	0.167	0.44	1500	189
650	691	730	0.167	0.455	1500	201.6
631	673	714	0.167	0.464	1500	209.16
605	649	691	0.167	0.477	1500	216.72
595	640	683	0.167	0.481	1500	221.76

Table 3.8: Observations: Temperature measurement using Johnson noise.

Using the Table 3.8 and Fig. 3.16, we see that we can derive a linear relationship between V10 and Average temperature. The straight line fit gives us the required equation for modeling.

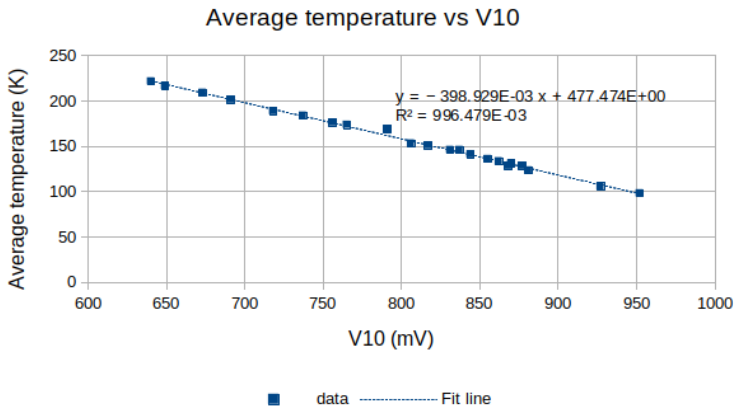

Figure 3.16: Plot of Average temperature vs V10.

The slope and intercept of Fig. 3.16 are (-0.399 ± 0.005)$\frac{K}{mV}$ and (477.5 ± 4.278)K respectively. We thus get the following relation (In Kelvin):

$$T = -0.399 \times V10 + 477.474 \tag{3.1}$$

3.6 Measurement of Boltzmann's Constant

Taking the relevant data, we will find the Boltzmann's constant. The electrical circuit remains the same as what was used in the previous section. We set R_f = 1kΩ, time constant = 1s at room temperature (298K). Only difference between this section and Section 3.4 is that we obtained a plot of effective bandwidth vs Johnson noise for a fixed R_{IN} in Section 3.4; here we do the same thing but for multiple R_{IN} values.

Bandwidth (Hz)	Effective Bandwidth (Hz)	$<V_J^2>$for different R_{IN}s (V^2)			
		R_{IN} = 1kΩ	R_{IN} = 3kΩ	R_{IN} = 10kΩ	R_{IN} = 30kΩ
320	355	6.667E-15	1.889E-14	5.667E-14	1.700E-13
300	333	4.444E-15	1.556E-14	5.444E-14	1.644E-13
230	258	4.444E-15	1.444E-14	4.556E-14	1.289E-13
30	105	1.111E-15	5.556E-15	1.778E-14	5.444E-14
0	9	0.000E+00	0.000E+00	0.000E+00	4.444E-15
0	0.4	0.000E+00	0.000E+00	0.000E+00	0.000E+00
990	1100	1.775E-14	5.401E-14	1.822E-13	5.444E-13
970	1077	1.852E-14	5.247E-14	1.778E-13	5.356E-13
900	1000	1.775E-14	5.170E-14	1.667E-13	5.011E-13
700	784	1.312E-14	3.781E-14	1.300E-13	3.967E-13
0	278	4.630E-15	1.466E-14	4.778E-14	1.411E-13
0	28	1.543E-15	3.086E-15	5.556E-15	1.444E-13
3290	3654	6.250E-14	1.836E-13	6.156E-13	1.833E-12
3270	3632	6.096E-14	1.806E-13	6.156E-13	1.833E-12
3200	3554	6.096E-14	1.798E-13	6.044E-13	1.799E-12
3000	3332	5.787E-14	1.698E-13	5.644E-13	1.708E-12
2300	2576	4.244E-14	1.312E-13	4.389E-13	1.333E-12
300	1051	1.852E-14	5.401E-14	1.833E-13	5.486E-13
9990	11096	1.900E-13	5.538E-13	1.852E-12	3.000E-12
9970	11074	1.867E-13	5.538E-13	1.852E-12	2.988E-12
9900	10996	1.856E-13	5.521E-13	1.840E-12	2.926E-12
9700	10774	1.833E-13	5.399E-13	1.802E-12	2.741E-12
9000	9997	1.678E-13	4.965E-13	1.679E-12	2.049E-12
7000	7839	1.300E-13	3.941E-13	1.321E-12	4.012E-12
32990	36643	6.296E-13	1.840E-12	6.259E-12	1.878E-11
32970	36620	6.296E-13	1.840E-12	6.272E-12	1.881E-11
32900	36543	6.235E-13	1.840E-12	6.247E-12	1.872E-11
32700	36321	6.235E-13	1.827E-12	6.210E-12	1.869E-11
32000	35543	6.142E-13	1.778E-12	6.074E-12	1.831E-11
30000	33324	5.772E-13	1.679E-12	5.728E-12	1.725E-11
99990	111061	1.914E-12	5.639E-12	1.933E-11	5.600E-11
99970	111039	1.901E-12	5.611E-12	1.928E-11	5.600E-11
99900	110961	1.901E-12	5.611E-12	1.925E-11	5.600E-11
99700	110739	1.901E-12	5.583E-12	1.928E-11	5.578E-11
99000	109961	1.877E-12	5.556E-12	1.914E-11	5.556E-11
97000	107740	1.852E-12	5.444E-12	1.886E-11	5.478E-11

Table 3.9: Observations: For measurement of Boltzmann's constant.

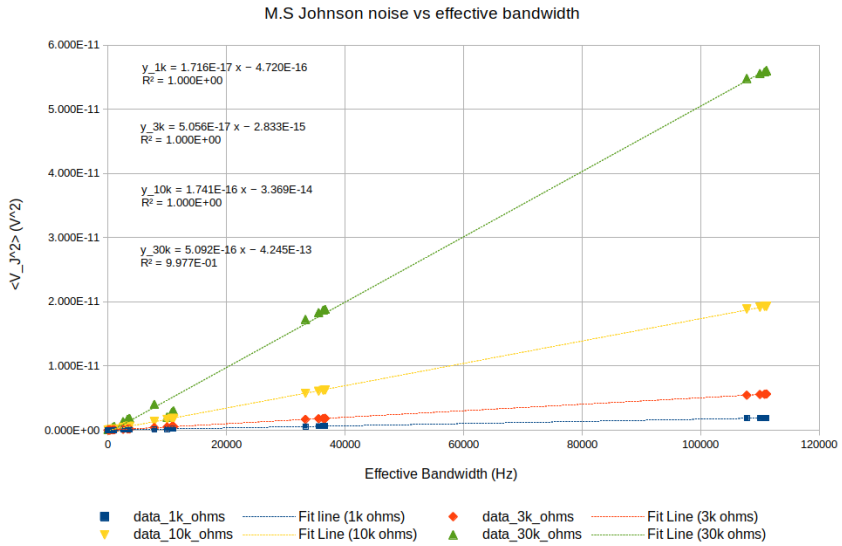

Figure 3.17: M.S Johnson noise vs effective bandwidth plot for different R_{IN}s.

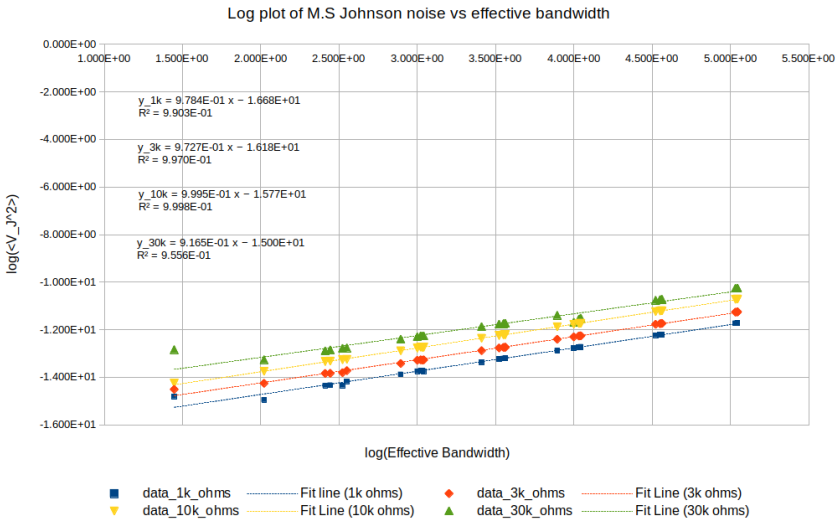

Figure 3.18: Log plot of M.S Johnson noise vs effective bandwidth for different R_{IN}s.

The slope and intercept of Fig. 3.17 and Fig. 3.18 are in the following tables respectively:

R_{IN}	Slope ($\frac{V^2}{Hz}$)	Error in slope ($\frac{V^2}{Hz}$)	Y-Intercept (V^2)	Error in Y-Intercept (V^2)
1kΩ	1.72E-17	1.316E-020	-4.71E-16	6.258E-16
3kΩ	5.056E-17	2.945E-20	-2.792E-15	1.4E-15
10kΩ	1.741E-16	2.034E-19	-3.369E-14	9.669E-15
100kΩ	5.092E-16	4.183E-18	-4.245E-13	1.988E-13

Table 3.10: Slopes, Y-Intercepts and the errors of the same for lines in for Fig. 3.17.

R_{IN}	Slope	Error in slope	Y-Intercept	Error in Y-Intercept
1kΩ	1.019E+00	8.000E-03	-1.685E+01	3.100E-02
3kΩ	9.974E-01	2.688E-03	-1.629E+01	1.066E-02
10kΩ	1.007E+00	1.750E-03	-1.580E+01	6.941E-03
100kΩ	9.920E-01	2.301E-02	-1.531E+01	9.125E-02

Table 3.11: Slopes, Y-Intercepts and the errors of the same for lines in for Fig. 3.18.

The slopes are essentially $V_J^2/\Delta f$ for different R_{IN}s. We now have the following table:

Noise Density (V^2/Hz)	R_{IN} (kΩ)
1.72E-17	1
5.06E-17	3
1.74E-16	10
5.09E-16	30

Table 3.12: Observations: Noise density vs R_{IN}.

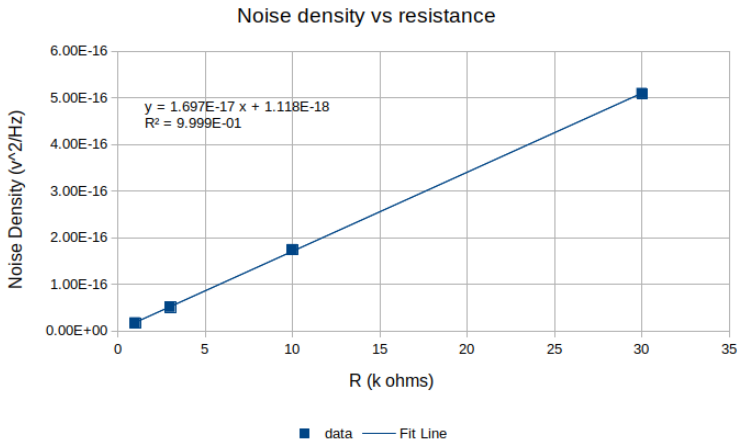

Figure 3.19: Plot of noise density vs R_{IN}.

The slope and intercept of the fitted line in Fig. 3.19 are $(1.696\times10^{-17} \pm 1.167\times10^{-19})\frac{V^2}{Hz\times k\Omega}$ and $(1.156\times10^{-18} \pm 1.855\times10^{-18})\frac{V^2}{Hz}$ respectively.

According to Eqn. 2.1, the slope of a plot of noise density vs R should give us $4k_BT$. Therefore from Fig. 3.19, we get (note that J = Ω.A^2.s):

$$k_B = \frac{slope}{4T} = (1.43 \times 10^{-23} \pm 1.098 \times 10^{-25})JK^{-1}$$

The error in k_B was found using the error in slope of the fitted line in Fig. 3.19 and that the error in Temperature measurement is the least count of the device used to measure the temperature, i.e 1K.

3.7 Dependence of Shot Noise on Photo-Diode Current and Bandwidth

Fig. 3.20 describes a circuit that has been optimized for measuring shot noise, and thus to determine the electronic charge, e.

The photo-diode current can be said to be $i(t) = i_{\rm dc} + \delta i(t)$ i.e. the sum of a d.c. average current plus the current fluctuations representing shot noise. By Ohm's law, this can be converted to $V_{\rm out}\,(t) = (-1)i_{\rm dc}R_{\rm f} + (-1)\delta i(t)R_{\rm f}$ In the a.c.-coupled path, we have 100 -fold voltage amplification, so the cable connecting the pre-amp output to the high-level electronics will be conveying the voltage signal $V_{\rm pre}\,(t) = 100{\rm x}(-1)R_{\rm f}\delta i(t)$ which will be devoid of any DC signal.

On further passing the signal through the squarer and taking time average, we can get

$$< V_{\rm sq}(t) >=< \delta i^2(t) > (100G_2R_{\rm f})^2\,/(10\text{ V})$$

We now have (using Eqn. 2.2):

$$< V_{\rm sq}(t) >= 2ei_{\rm dc}\Delta f\,(100G_2R_{\rm f})^2\,/(10\text{ V}) \tag{3.2}$$

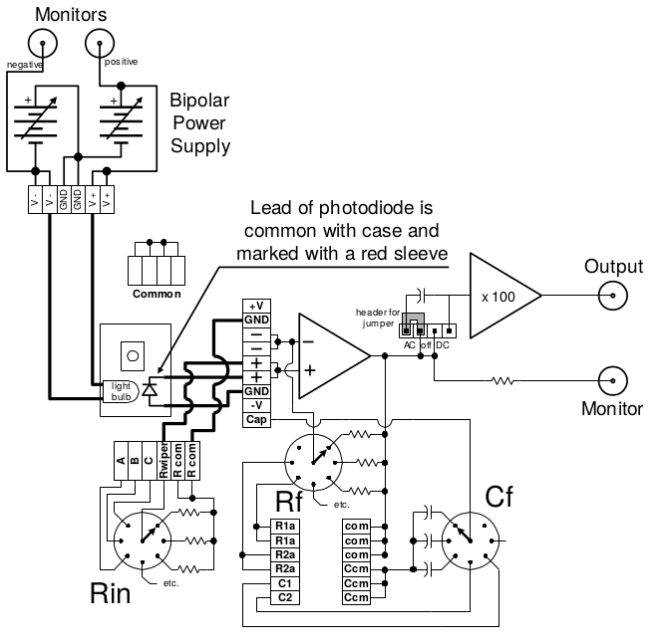

Figure 3.20: Circuit used for shot noise measurements. Source: [1].

A multimeter is connected to the "MONITOR" point on the panel of the pre-amp. We get $V_{mon} = (-)i_{dc}R_f$. This gives us the value of i_{dc}. In all these equations G_2 is the HLE gain.

We first verify Eqn. 3.2 for the linear dependence of V_{sq} on photo-diode current and then on bandwidth for 2 different light sources: red LED and an IR LED.

3.7.1 V_{sq} vs Photo-Diode Current

For the measurements in this sub-section, we use time constant = 1s, R_f = 10kΩ (which means LLE gain = 100), bandwidth = (1-100)kHz. We refer to the voltage from the pre-amp monitor as V_{in}, the final squarer voltage as V_{out}. V_{in} offset = -0.3mV.

V_{in} (mV)	V_{out} (V)	Gain (G1×G2)	Amplification Noise (V)	Corrected V_{out} (V)	Corrected V_{in} (mV)	i_{dc} (nA)
-5	0.497	400000	0.469	0.028	-4.7	500
-10	0.527	400000	0.469	0.058	-9.7	1000
-15	0.558	400000	0.469	0.089	-14.7	1500
-20	0.588	400000	0.469	0.119	-19.7	2000
-25	0.619	400000	0.469	0.15	-24.7	2500
-30	0.65	400000	0.469	0.181	-29.7	3000
-35	0.683	400000	0.469	0.214	-34.7	3500
-40	0.715	400000	0.469	0.246	-39.7	4000
-45	0.747	400000	0.469	0.278	-44.7	4500
-50	0.779	400000	0.469	0.31	-49.7	5000
-55	0.81	400000	0.469	0.341	-54.7	5500
-60	0.841	400000	0.469	0.372	-59.7	6000
-65	0.873	400000	0.469	0.404	-64.7	6500
-70	0.905	400000	0.469	0.436	-69.7	7000

Table 3.13: Observations: Shot noise measurements for red LED.

V_{in} (mV)	V_{out} (V)	Gain (G1×G2)	Amplification Noise (V)	Corrected V_{out} (V)	Corrected V_{in} (mV)	V_{in}× Gain^2	Gain^2 × i_{dc} (nA)
-50.9	0.775	400000	0.472	0.303	-50.6	-8.096E+12	8.096E+14
-100.1	0.6	300000	0.265	0.335	-99.8	-8.982E+12	8.982E+14
-150.7	0.77	300000	0.265	0.505	-150.4	-1.354E+13	1.354E+15
-199.8	0.935	300000	0.265	0.67	-199.5	-1.796E+13	1.796E+15
-250.6	0.49	200000	0.117	0.373	-250.3	-1.001E+13	1.001E+15
-299.3	0.563	200000	0.117	0.446	-299	-1.196E+13	1.196E+15
-350.3	0.64	200000	0.117	0.523	-350	-1.400E+13	1.400E+15
-400.4	0.715	200000	0.117	0.598	-400.1	-1.600E+13	1.600E+15
-450	0.791	200000	0.117	0.674	-449.7	-1.799E+13	1.799E+15
-500	0.865	200000	0.117	0.748	-499.7	-1.999E+13	1.999E+15

Table 3.14: Observations: Shot noise measurements for IR LED.

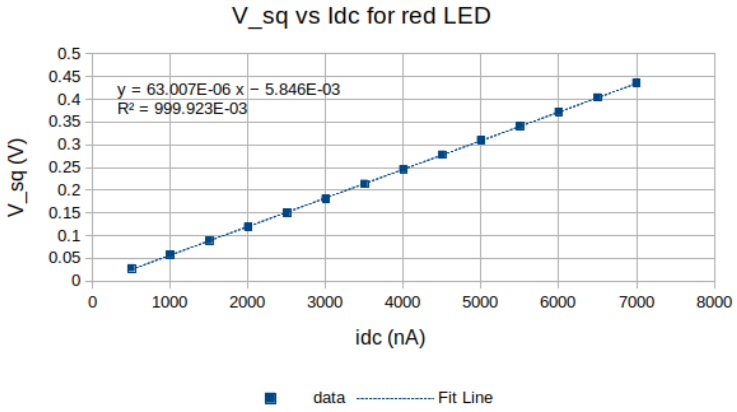

Figure 3.21: V_{sq} vs i_{dc} for red LED.

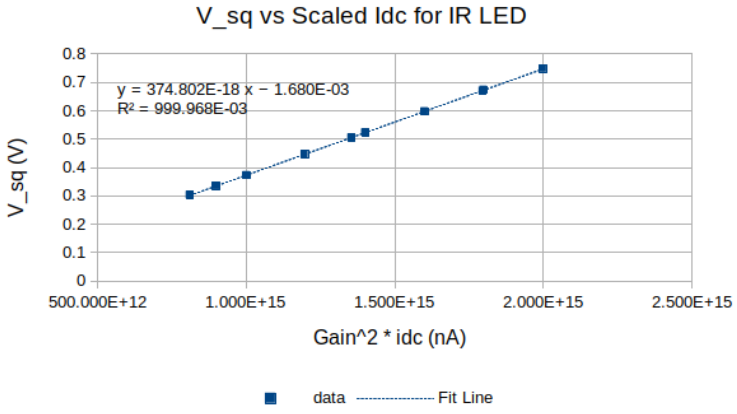

Figure 3.22: V_{sq} vs Gain^2× i_{dc} for IR LED.

The X-Axis of Fig. 3.22 is scaled by the (Gain)^2 because we used different gains for different readings and in order to obtain e from this plot we were required to make this change.

The slope and intercept of the fitted line in Fig. 3.21 are $(6.301\times10^{-5} \pm 1.592\times10^{-7})\frac{V}{nA}$ and $(-5.846\times10^{-3} \pm 6.778\times10^{-4})$V respectively. The same for Fig. 3.22 are $(3.747\times10^{-16} \pm 7.646\times10^{-19})\frac{V}{nA}$ and $(-1.572\times10^{-3} \pm 1.1\times10^{-3})$V respectively.

3.7.2 V_{sq} vs Bandwidth

For the measurements in this sub-section, we use time constant = 1s and R_f = 10kΩ (which means LLE gain = 100). We refer to the voltage from the pre-amp monitor as

V_{in}, the final squarer voltage as V_{out}. V_{in} offset = -0.3mV.

Bandwidth (kHz)	V_{out} (V)	Gain (G1×G2)	Amplification Noise (V)	Corrected V_{out} (V)	Effective bandwidth (kHz)	$\frac{\text{Corrected } V_{out}}{Gain^2}$ (V)	i_{dc} (mA)
100	0.78	400000	0.471	0.309	111.061	1.931E-12	4970
33	0.563	600000	0.334	0.229	36.643	6.361E-13	4970
10	0.283	800000	0.164	0.119	11.096	1.859E-13	4970
3.3	0.075	800000	0.042	0.033	3.654	5.156E-14	4970
1	0.007	800000	0.003	0.004	1.1	6.250E-15	4970
0.33	0	800000	0	0	0.355	0.000E+00	4970

Table 3.15: Observations: Shot noise measurements for red LED. V_{in} = -50+0.3 mV.

Bandwidth (kHz)	V_{out} (V)	Gain (G1×G2)	Amplification Noise (V)	Corrected V_{out} (V)	Effective bandwidth (kHz)	$\frac{\text{Corrected } V_{out}}{Gain^2}$ (V)	i_{dc} (mA)
100	0.935	300000	0.265	0.67	111.061	7.444E-12	19970
33	0.844	500000	0.237	0.607	36.643	2.428E-12	19970
10	0.647	800000	0.18	0.467	11.096	7.297E-13	19970
3.3	0.214	800000	0.06	0.154	3.654	2.406E-13	19970
1	0.063	800000	0.017	0.046	1.1	7.188E-14	19970
0.33	0.02	800000	0.005	0.015	0.355	2.344E-14	19970

Table 3.16: Observations: Shot noise measurements for IR LED. V_{in} = -200+0.3 mV.

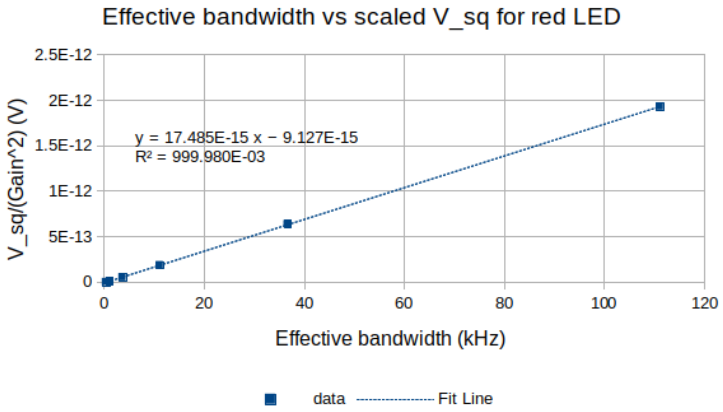

Figure 3.23: $V_{sq}/(\text{Gain})^2$ vs effective bandwidth for red LED.

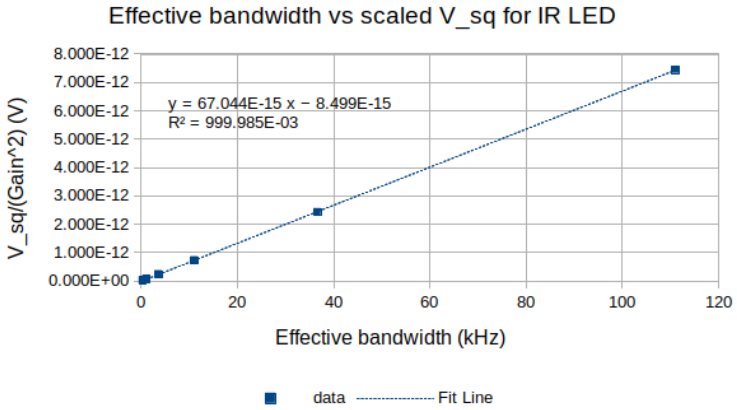

Figure 3.24: $V_{sq}/(\text{Gain})^2$ vs effective bandwidth for IR LED.

The Y-Axis of Figs. 3.23 and 3.24 are scaled by the Gain^2 because we used different gains for different readings and in order to obtain e from this plot we were required to make this change.

The slope and intercept of the fitted line in Fig. 3.23 are $(1.748\times10^{-14} \pm 3.948\times10^{-17})\frac{V}{kHz}$ and $(-9.118\times10^{-15} \pm 1.894\times10^{-15})$V respectively. The same for Fig. 3.24 are $(6.704\times10^{-14} \pm 1.278\times10^{-16})\frac{V}{kHz}$ and $(-8.466\times10^{-15} \pm 6.133\times10^{-15})$V respectively.

3.8 Measurement of e

For red and IR LEDs we have two plots each to calculate the value of e using Eqn. 3.2. Hence, we have the following results:

Plot	Red LED	IR LED
V_{sq} vs I_{dc}	$(1.79\times10^{-19} \pm 8.028\times10^{-21})$C	$(1.687\times10^{-19} \pm 6.764\times10^{-21})$C
V_{sq} vs effective bandwidth	$(1.759\times10^{-19} \pm 6.569\times10^{-22})$C	$(1.679\times10^{-19} \pm 5\times10^{-22})$C

Table 3.17: Results: Measurement of the fundamental unit of charge, e.

Note that some plots had the V_{sq} or I_{dc} scaled by $(\text{Gain})^2$ which has not been reflected in the names given to the plots in column 2 of Table 3.17.

The errors in the value of e were found using the following known points (most of which are from [1]:

1. All the gain-critical resistors are of 0.1% precision, so the overall gain can be trusted at the 1% level.
2. R_f and R_{IN} values have tolerances of 0.1% upto 1MΩ, and 1% thereafter.
3. Error in V_{sq} is the least count, 0.1mV.
4. Error in $i_{dc} = <V_{sq}>/R_{IN}$ was calculated from errors in the voltage and resistance.
5. The effective gain values are all subject to uncertainties of order 4%.

3.9 Diagnosing Proper High-Frequency Behavior

This section aims to check the 'gain flatness' of your pre-amplifier section, and to compensate for the 'gain peaking' that tends to occur in the neighborhood of f >2 MHz because of capacitive effects in the photo-diode and the pre-amp's first stage. Up to this point we have assumed that the current-to-voltage converter of the previous section exhibits a conversion coefficient R_f which is frequency-independent. This is important, because while the d.c. value of this conversion coefficient relates i_{dc} to V of the pre-amp monitor, it's the behavior of this coefficient at (and well beyond) frequencies of 100 kHz which applies to the various frequency components of the noise we're measuring. Apart from the TeachSpin apparatus, we will be using a function generator to have control over the frequencies and the corresponding intensity. Fig. 3.25 shows the circuits involved in this experiment. For the experiments we conduct, we will be using the square-wave function of the signal generator.

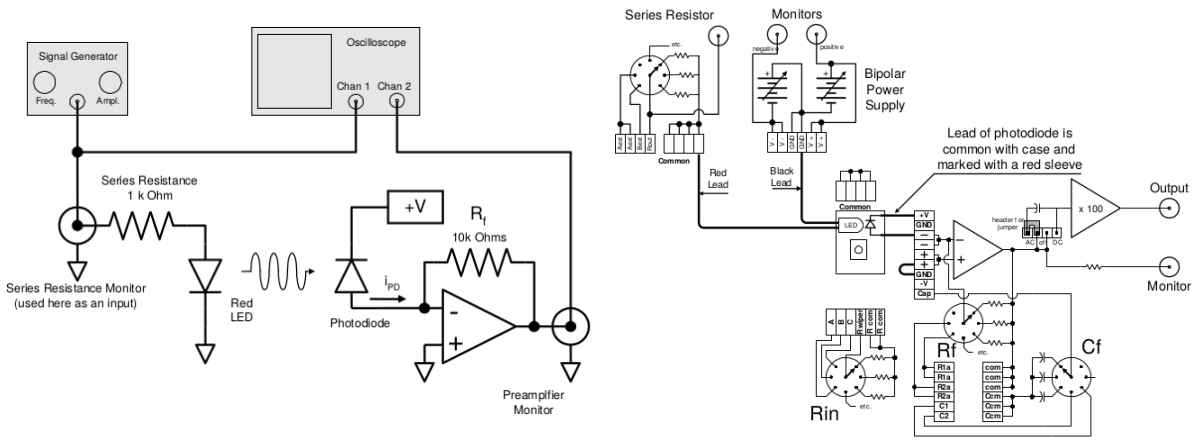

(a) (b)

Figure 3.25: Circuits for studying high-frequency behavior. Source: [1]

A square-wave drive can cause the LED to alternate, at any desired rate, between off and on states. An oscilloscope looking at your pre-amp's Monitor point will show you the direct-coupled version of the photo-current resulting from your modulated LED output. The following images show the input signal (blue) and the response from the pre-amp monitor (yellow):

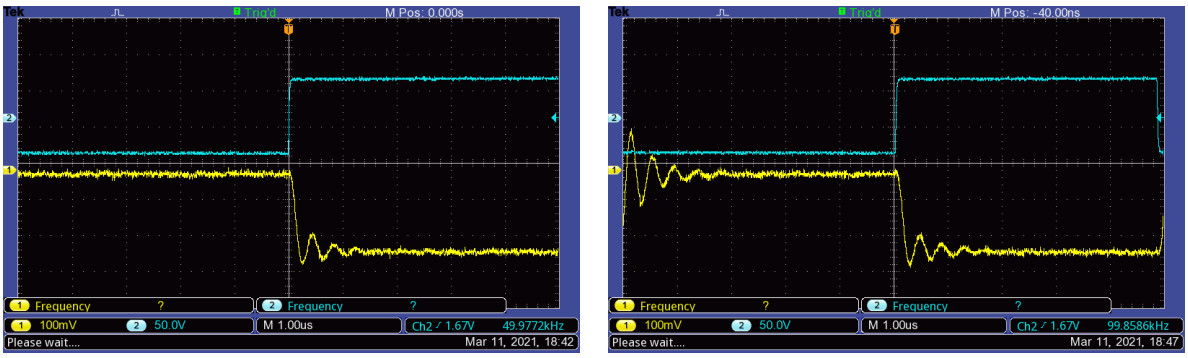

(a) (b)

Figure 3.26: Observations: (a) 50kHz and (b) 100kHz source and their response.

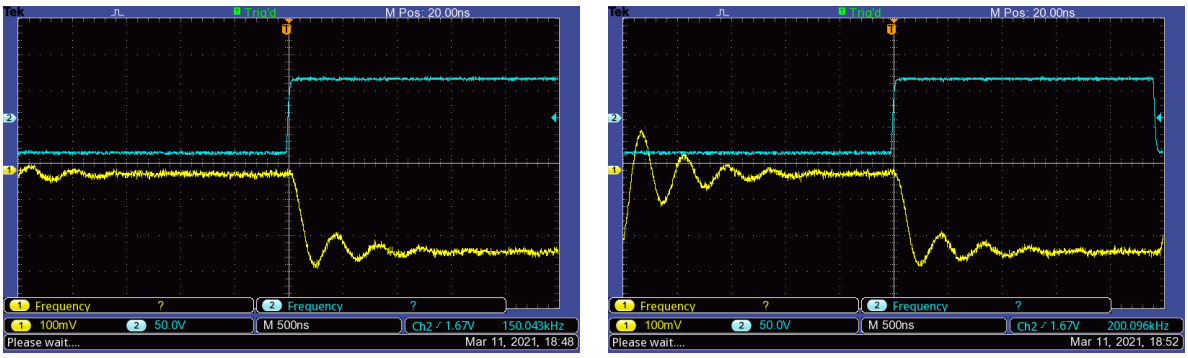

(a) (b)

Figure 3.27: Observations: (a) 150kHz and (b) 200kHz source and their response.

We observe that there is a ringing effect in the response of the images above. The only new component needed to reduce this ringing problem is by adding a feedback capacitor, connected in parallel with the feedback resistor seen in Fig. 3.25a. Thus the subsequent wiring would be as seen in Fig. 3.28.

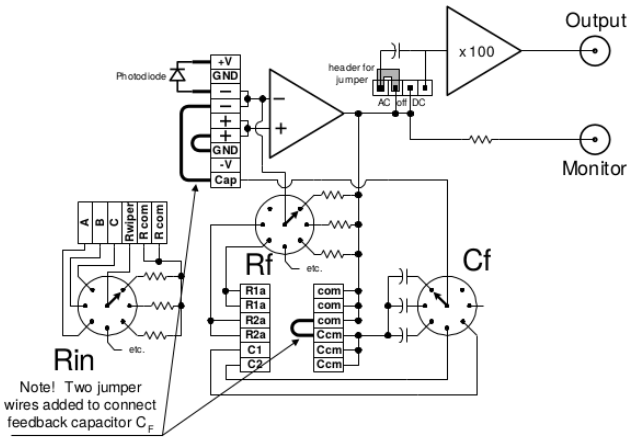

Figure 3.28: Observations: Circuit for reducing gain peaking. Source: [1]

After this addition, for an input square wave of frequency 250Hz, we get the following results:

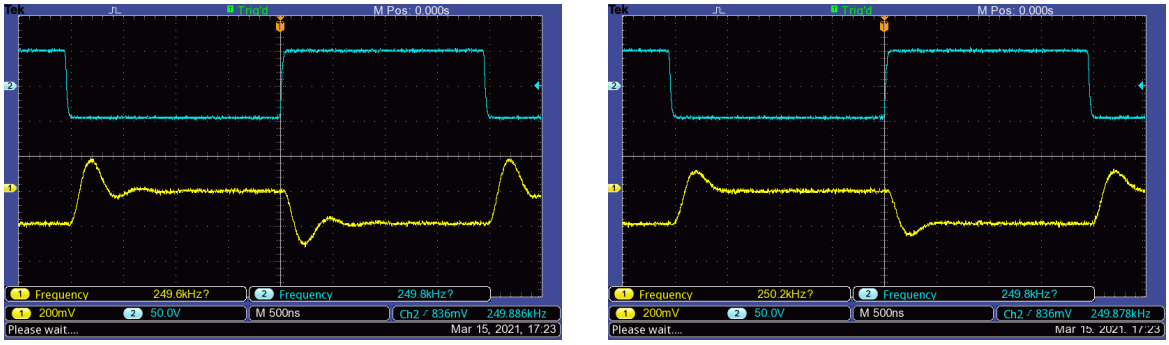

(a) (b)

Figure 3.29: Observations: Source and Response for (a) minimum value and (b) 3.3pf capacitors.

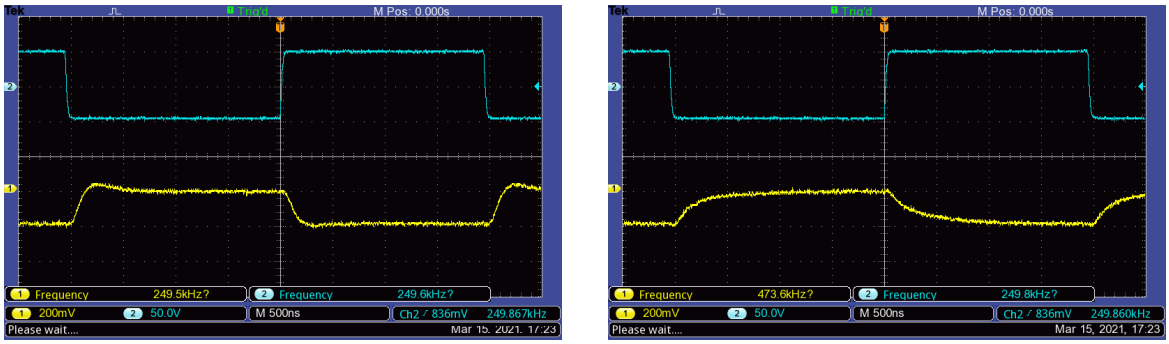

(a) (b)

Figure 3.30: Observations: Source and Response for (a) 10pf and (b) 33pf capacitors.

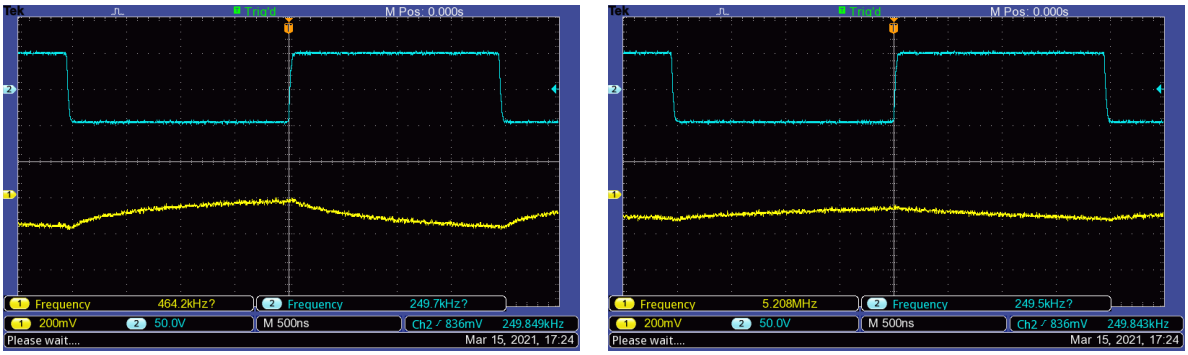

(a) (b)

Figure 3.31: Observations: Source and Response for (a) 100pf and (b) 330pf capacitors.

The efficiency in removal of this gain peaking seems to be directly proportional to the magnitude of capacitance used in the setup, but ofcourse we also see a tendency to lose the characteristics of the square wave itself.

3.10 Sub-Shot Noise

This section would involve producing and quantifying a sub-shot-noise current. Figure 3.32 shows the schematic diagram for the input of the circuit.

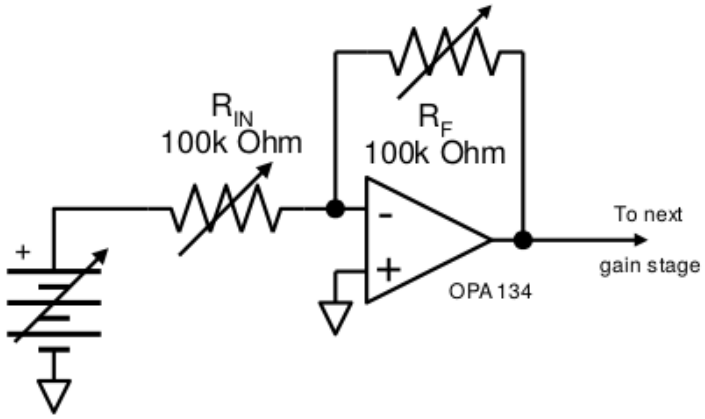

Figure 3.32: Observations: Schematic diagram of a circuit for sub-shot noise. Source: [1]

For the experiment, we had time constant = 1s, bandwidth = (1-100)kHz, LLE gain = 100, conducted at room temperature (296K).

Bipolar voltage (V)	Pre-amp monitor voltage (V)	$<V_{sq}>$ (mV)	HLE Gain
0.003	-0.003	109.8	500
6	-6	109.8	500

Table 3.18: Observations: Sub-shot noise measurements.

We see that the amplification gain (corresponding to Bipolar voltage supply = 0) and the next reading is the same which means that we observe no sub-shot currents. We looked at voltages up to the milli-volt range, but there is a possibility that these currents correspond to a voltage of magnitude under the milli-volt range.

Chapter 4

Errors Involved and Conclusive Remarks

This chapter will cover the results of all the experiments explained in Chapter 3 in the respective order they were described. The error values for all numbers we calculated were already presented in the previous Chapter, they were found using (for a function f = f(x,y)):

$$\delta f = \sqrt{(\frac{\partial f}{\partial x} \times \delta x)^2 + (\frac{\partial f}{\partial y} \times \delta y)^2} \tag{4.1}$$

As explained in Section 3.8, R_f and R_{IN} values have tolerances of 0.1% upto 1MΩ, and 1% thereafter.. Since all gain-critical resistors are of 0.1% precision, so the overall gain can be trusted at the 1% level. The error in V_{sq} is the least count of the multimeter, 0.1mV. And finally, the effective bandwidth values are all subject to uncertainties of order 4%. The tolerances of these four values account for all errors in measurements we took throughout this experiment.

4.1 Precautions and Sources of Errors

Common precautionary measures to be aware of, while performing the set of experiments in this report:

- The bulb, LED and photo-diode have very fragile wire connections, make sure you handle them carefully.
- Liquid Nitrogen is a dangerous substance, make sure you take all safety precautions while handling it. It is better to have another colleague to tighten the dewar.
- Make sure the wire connections made in the interior of the LLE box are tight, they sometimes tend to easily come out if the screw is not tightened properly.
- Do not forget the 10V scaling factor while performing calculations involving the squarer voltage.
- Always use effective bandwidth instead of bandwidth, unless required.

Common sources of error we faced during the entirety of the experiment include:

- Adjust gain to make sure the squarer voltage output is always under 1V.
- Make sure your LEDs and light bulbs are powering up under a voltage supply. To check for IR LED, most smart phone cameras can now detect some wavelengths of IR light too.
- Under low temperatures, the remote resistances can produce different resistance values, check the same using the breakout box given with the TeachSpin, Inc. equipment.

All experiments we sought to do were completed on time, and additional experiments were also performed. To summarise, we have (performed) obtained the following (experiments) results:

- We empirically validated the existence of Johnson Noise.
- We showed that the M.S Johnson noise depended linearly on the resistance, bandwidth and temperature. Linear dependence on bandwidth empirically means that we are entitled to infer the existence of 'noise density'.
- We also showed we can model and measure the temperature through the setup we used.
- By plotting noise density vs resistance, we found that the Boltzmann's constant to be $1.43\times10^{-23} \pm 1.098\times10^{-25}\text{JK}^{-1}$.
- We showed that shot noise depended linearly on photo-diode current and bandwidth.
- Through the four plots obtained from the above point, we obtained the value of the fundamental unit of charge, e:

Plot	Red LED	IR LED
V_{sq} vs I_{dc}	$(1.79\times10^{-19} \pm 8.028\times10^{-21})$C	$(1.687\times10^{-19} \pm 6.764\times10^{-21})$C
V_{sq} vs effective bandwidth	$(1.759\times10^{-19} \pm 6.569\times10^{-22})$C	$(1.679\times10^{-19} \pm 5\times10^{-22})$C

- We checked the gain-flatness of the pre-amp section and how to correct for the ripples that were produced at high frequencies.
- Finally we looked into the existence of sub-shot noise currents, but unfortunately we were not able to observe any sub-shot currents. We looked at voltages up to the milli-volt range, but there is a possibility that these currents correspond to a voltage of magnitude under the milli-volt range.

4.2 Future Work

- Continuing from where we left off, one can look into sub-shot noise currents using instruments of lesser least count. There is also a possibility that we were doing something wrong, but nonetheless it would be interesting to know that there are noises of magnitude lesser than sub-shot noise.
- We go back to the temperature modelling and measurement (Section 3.5.2) where we showed the possibility of generating and measuring multiple temperature points

using the setup that was given to us. Continuing from here, one can measure Johnson noise at these temperatures, which compared to the two-temperature Johnson noise measurement, is more than 2 data points points (77K and room temperature).

- Apart from the above two suggestions, the experiments we performed form a closed set of experiments. Other future work can include conducting newer sections of experiments given in the TeachSpin, Inc. manual, there were many experiments that we could not get our hands on in the given time frame we were provided with.

Bibliography

[1] David Van Baak. *Noise Fundamentals*. 2010 (pages 4–7, 10, 11, 13, 18, 25, 28–31).

[2] MIT Department of Physics. *Johnson Noise and Shot Noise: The Determination of the Boltzmann Constant, Absolute Zero Temperature and the Charge of the Electron*. Tech. rep. Massachusetts Institute of Technology, Sept. 2013, p. 15. URL: http://web.mit.edu/8.13/www/JLExperiments/JLExp43.pdf (page 5).

[3] Bernd Schröder. "The Poisson Distribution". Louisiana Tech University, College of Engineering and Science. URL: http://www.math.usm.edu/schroeder/slides/stat/Poisson_dist.pdf (page 38).

Appendix A

Derivation of the Johnson-Nyquist Equation

Any resistor connected with its two terminals will have some value of capacitance associated with it. Energy inside a capacitor is given by

$$E = \frac{1}{2}CV^2$$

This potential energy inside the capacitor determines the kinetic energy of thermal motion of charges. The thermal motion of these charges can be characterized by energy distribution of charges with temperature. For an electronic energy of charges, it can be depicted by the voltage across resistor. Now from the Boltzmann's energy distribution the probability of finding the voltage between V and $(V + dv)$ is given by

$$dP = K_o e^{\frac{-CV^2}{2k_B^T}} dV$$

Where K_o is just normalization constant and k_B is Boltzmann's constant. Now for calculation of normalization constant: Make substitution

$$x^2 = \frac{CV^2}{2k_BT}, \quad 2xdx = \frac{C}{2k_BT}2VdV, \quad dV = \frac{2k_BT}{C}\frac{x}{V}dx$$
$$dV = \sqrt{\frac{2k_BT}{C}}dx$$

By setting the integrated probability to be 1.

$$K_o\sqrt{\frac{2k_BT}{C}}\underbrace{\int_{-\infty}^{\infty} e^{-x^2}dx}_{\sqrt{\pi}} = 1 \Longrightarrow K_o = \sqrt{\frac{C}{2\pi k_BT}}$$

Then the quantity we can observe during experiment is mean squared value of voltage we need to calculate $\bar{V}^2$.

$$\overline{V^2} = \sqrt{\frac{C}{2\pi k_BT}}\int_{-\infty}^{\infty} V^2 \exp\left(-\frac{CV^2}{2k_BT}\right) dV$$

Variable substitution and Gaussian integral gives voltage between V and $(V+dv)$ is given by

$$dP = K_o e^{\frac{-CV^2}{2k_BT}} dV$$

Where K_o is just normalization constant and k_B is Boltzman constant. Now for calculation of normalization constant: Make substitution

$$x^2 = \frac{CV^2}{2k_BT}, \quad 2xdx = \frac{C}{2k_BT}2VdV, \quad dV = \frac{2k_BT}{C}\frac{x}{V}dx$$
$$dV = \sqrt{\frac{2k_BT}{C}}dx$$

By setting the integrated probability to be 1.

$$K_o\sqrt{\frac{2k_BT}{C}}\underbrace{\int_{-\infty}^{\infty} e^{-x^2}dx}_{\sqrt{\pi}} = 1 \Longrightarrow K_o = \sqrt{\frac{C}{2\pi k_BT}}$$

Then the quantity we can observe during experiment is mean squared value of voltage we need to calculate $\bar{V^2}$.

$$\overline{V^2} = \sqrt{\frac{C}{2\pi k_BT}}\int_{-\infty}^{\infty} V^2 \exp\left(-\frac{CV^2}{2k_BT}\right)dV$$

Variable substitution and Gaussian integral gives

$$\overline{V^2} = \sqrt{\frac{C}{2\pi k_BT}}\sqrt{\left(\frac{2k_BT}{C}\right)^3}\underbrace{\int_{-\infty}^{\infty} x^2e^{-x^2}dx}_{\sqrt{\pi/2}}$$

$$\overline{V^2} = \frac{k_BT}{C}$$

Calculation for $\overline{V^2}$ in a frequency range : Define $S_V(0)df$ as the mean squared voltage of the source V_N per interval of frequency Now voltage across the resistor and capacitor model we have taken

$$d\overline{V_c^2} = S_V(0)df\frac{(\omega C)^{-2}}{R^2+(\omega C)^{-2}} = \frac{S_V(0)df}{1+(\omega RC)^2}$$
$$\overline{V_c^2} = \int_0^{\infty} d\overline{V_c^2} = S_V(0)\int_0^{\infty}\frac{df}{1+(\omega RC)^2}$$
$$\overline{V_c^2} = \frac{SV(0)}{2\pi RC}\underbrace{\int_0^{\infty}\frac{dx}{1+x^2}}_{\pi/2}$$
$$\overline{V_c^2} = \frac{S_V(0)}{4RC}$$

Earlier we calculated $\overline{V^2}$ using thermodynamics and now using electronics across resistance which has capacitance C. Equating these we get

$$\overline{V_c^2} = \frac{S_V(0)}{4RC} = \frac{k_BT}{C}$$

and since $S_V(0) = \overline{V^2}/\Delta f$ the expression for Johnson noise in a resistor of resistance R at temperature T is given as

$$\overline{V^2} = 4k_BTR\Delta f$$

Δf is bandwidth in which the noise is measured and k_B is Boltzmann's constant.

Even if it has a dependence on effective bandwidth, spectrum of Johnson noise is uniform throughout the whole electronic bandwidth. This means that power spectral density of Johnson noise is independent of frequency. Because of this uniform spectrum, Johnson noise can be referred as white noise.

Appendix B

Derivation of Variance of a Poisson Distribution

As [3] explains, a random variable is said to have a Poisson distribution with parameter $\lambda > 0$ if and only if its probability mass function is $p(x;\lambda) = \frac{e^{-\lambda}\lambda^x}{x!}$

Expectation value of X:

$$E(X) = \sum_{x=0}^{\infty} x\frac{e^{-\lambda}\lambda^x}{x!} = \sum_{x=1}^{\infty} \frac{e^{-\lambda}\lambda^x}{(x-1)!} = \lambda e^{-\lambda} \sum_{x=1}^{\infty} \frac{\lambda^{x-1}}{(x-1)!} = \lambda e^{-\lambda} \sum_{j=0}^{\infty} \frac{\lambda^j}{j!} = \lambda e^{-\lambda} e^{\lambda} = \lambda$$

Expectation value of X^2:

$$E\left(X^2\right) = \sum_{x=0}^{\infty} x^2\frac{e^{-\lambda}\lambda^x}{x!} = \sum_{x=0}^{\infty} x(x-1)\frac{e^{-\lambda}\lambda^x}{x!} + \sum_{x=0}^{\infty} x\frac{e^{-\lambda}\lambda^x}{x!} = \sum_{x=2}^{\infty} x(x-1)\frac{e^{-\lambda}\lambda^x}{x!} + \lambda$$

$$= e^{-\lambda}\lambda^2 \sum_{x=2}^{\infty} \frac{\lambda^{x-2}}{(x-2)!} + \lambda = e^{-\lambda}\lambda^2 \sum_{k=0}^{\infty} \frac{\lambda^k}{k!} + \lambda = e^{-\lambda}\lambda^2 e^{\lambda} + \lambda = \lambda^2 + \lambda$$

We thus have variance:

$$V(X) = E\left(X^2\right) - E(X)^2 = \lambda^2 + \lambda - \lambda^2 = \lambda$$